

PAPER • OPEN ACCESS

Numerical modeling of eccentric mass rotation in chamber filled with fluid

To cite this article: AV Savchenko *et al* 2019 *IOP Conf. Ser.: Earth Environ. Sci.* **262** 012061

View the [article online](#) for updates and enhancements.



IOP | ebooks™

Bringing you innovative digital publishing with leading voices to create your essential collection of books in STEM research.

Start exploring the collection - download the first chapter of every title for free.

Numerical modeling of eccentric mass rotation in chamber filled with fluid

AV Savchenko*, DS Evstigneev and MN Tsupov

Chinakal Institute of Mining, Siberian Branch Russian, Academy of Sciences,
Novosibirsk, Russia

E-mail: *lion_ltd@ngs.ru

Abstract. Numerical modeling of eccentric mass rotation in fluid under different water and oil pressures is performed. The relationship of extra-consumed motor power to overcome fluid resistance in downhole operation of screw pump at the maximum design depth of n is obtained. The power consumption of vibration sources is evaluated in the productive field of low- and high-viscosity oil in Mongolia and Russia.

1. Introduction

Borehole mining method in oil production uses sucker-rod, electric-centrifugal or screw pumps. The application depth of sucker-rod pumps is limited to 1400 m. Deeper level oil recovery involves electric-centrifugal or screw pumps. The highest efficiency in well cleanout and flow rate stimulation is achieved with the method of vibro-treatment of wellbottom zone using downhole vibration sources [1–5]. The unbalance vibration source for downhole operation at depths greater than 1400 m with any available types of pumps is proposed in [6, 7]. The source generates harmonic vibrations due to unbalance mass of load moving relative to the shaft rotation axis and transmits them directly to reservoir. The inner chamber of the vibration source is unsealed, and fluid, entering the chamber from the well, prevents rotation of eccentric mass, which increases the pump motor load. This study aims at finding power consumption of downhole unbalance vibration source in recovery of different-type oil at a depth down to 2500 m.

2. Modeling rotation of eccentric mass in fluid

The downhole vibration source consists of an internal chamber, shaft and eccentric mass, and is placed at the occurrence depth of pay zone. The internal chamber is unsealed and filled with fluid. The eccentric mass is rotated by the shaft; it is made of steel in the form of a semicylinder rotating clockwise at an angular rate $\vec{\omega}$ about the axis Oz (Figure 1). In numerical modeling, the computational domain encompassing the eccentric mass and the internal chamber, $\Omega = \Omega_1 \cup \Omega_2$, is divided into two sub-domains: Ω_1 , in which the eccentric mass rotates, and the immobile sub-domain Ω_2 . Such approach was for the first time proposed in [8] and later on was named the method of Multiple Reference Frame—MRF [9–13]. Equations of hydrodynamics with steady-state flows are solved using one of numerical methods. The net domain remains static, i.e., the net is unchanged during the calculation. In the sub-domain holding the rotating eccentric mass, the equations of fluid flow and continuity include the angular rate $\vec{\omega}$. In the immobile sub-domain, in the equation of motion, inertia forces are neglected and fluid mass transfer at the boundary of two domains is set as the equality of fluid pressures and normal



component of absolute velocity. At the boundary of the immobile sub-domain Ω_2 and inface of the chamber, sliding condition is set [14–16], and modeling of flows in the boundary layer at the hard surface of the eccentric mass in the sub-domain Ω_1 uses well functions [17].

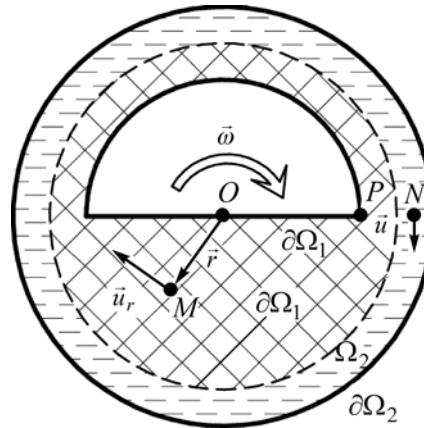
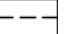




Figure 1. Arrangement of eccentric mass in fluid-filled chamber of vibration source: line  marks the boundary between Ω_1  in which eccentric mass rotates and Ω_2  at the chamber wall.

Rotation axis of the eccentric mass passes through the point O , middlelength section of the eccentric mass blade— OP ; the the points M and N , fluid flow velocities are directed along the vectors \vec{u}_r and \vec{u}_t , respectively, the points O and M are connected by the radius vector \vec{r} .

3. Modeling results of vibration source operation in water

Let us set water pressure in well in the range from 0.101325 to 25 MPa with an increment of 5 MPa and calculate change in density and dynamic viscosity versus depth. The results are compiled in the table below.

Table 1. Change in density and dynamic viscosity of water with increasing depth.

Pressure, MPa	Depth, m	Density, kg/m ³	Dynamic viscosity, 10 ⁻⁶ Pa·s
0.101325	0	998.2	1003
5	509.6	1000.6	1000
10	1016.7	1003.0	998.1
15	1521.4	1005.4	996.1
20	2023.7	1007.8	994.2
25	2523.6	1010.2	992.3

The power required for the motor to overcome the fluid resistance during operation of the unbalance vibration source at different depth is assessed is given by [14, 16]:

$$P = 2\pi f \Delta T_q, \quad (1)$$

where f is the rotation frequency of the eccentric mass, Hz; ΔT_q is the difference of the moments of forces; T_q is the moment of force, N, found by integrating pressure distribution on the middlelength section of the eccentric mass blade with a diameter D and a length L [16]:

$$T_q = \iint_S \vec{r} \times p(x, y) d\vec{\sigma} = L \int_0^{D/2} p(r) r dr. \quad (2)$$

The pressure distribution $p(p)$ on the blade of the eccentric mass is determined from numerical solution of equations of hydrodynamics with rotating sub-domain. The input parameters for the dynamic

model are taken from the table above. The rotation frequency of the eccentric mass is assumed as 5 Hz. The calculations in ANSYS Fluid Flow (Fluent) used the Reynolds-averaged Navier–Stokes equations with the standard two-parameter k – ε model of turbulence for steady-state flows [16, 17, 20, 21]. Figure 2 shows the relationship between the power intake of the motor in overcoming of water resistance during operation of the unbalance vibration source at different depths.

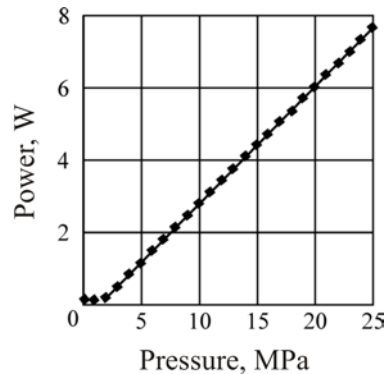


Figure 2. Power consumption as function of pressure in well at various depths (points show the calculated values, solid line is the linear interpolation).

Aiming to analyze influence of oil viscosity and density on motor load in rotation of the eccentric mass, two reservoirs of low-viscosity light and high-viscosity heavy oil are selected.

Verkh-Tarskoe field lies in the north of the Novosibirsk Region, 340 km away from Novosibirsk. The oil-bearing stratum U_1^1 with the average occurrence depth of 2455.6–2530.4 m contains light (density $< 850 \text{ kg/m}^3$) low-viscosity ($260 \cdot 10^{-6}$ – $780 \cdot 10^{-6} \text{ Pa}$) oil with small content of sulfur 0.3% and paraffine 1.81% [22]. The operation of the unbalance vibration source at the occurrence depth of the producing stratum IO_1^1 at the well pressure of 23.9 MPa will take 7.43 W to overcome head resistance of oil on the eccentric mass blade and 7.29 W in case that the well is filled with water.

Tsagaan-Els oilfield is located in the south-east of Mongolia, in the East Gobi basin. This is a sandwich-type reservoir represented by a number of producing blocks with tectonic and lithological partings. The main pay zone is from 1000 to 2500 m deep. Oil is highly paraffinic and contains not less than 11% by mass of solid hydrocarbons and not more than 0.2% by mass of sulfur. Well No. 1410 produces viscous ($178040 \cdot 10^{-6} \text{ Pa}\cdot\text{s}$) heavy oil (density 921.2 kg/m^3) at a depth of 1170 m [23]. The power to be consumed to overcome head resistance of oil is 8.75 W and 3.24 W in the well filled with water.

4. Discussion

It follows from the relationship between the power consumption and well pressure in Figure 2 that there is almost no increment in the power intake down to the depth of 306 m as the dynamic viscosity of water changes insignificantly. Starting from the pressure of 3 MPa, the power consumption grows by the linear law with a slope of 0.327 and initial ordinate -0.527 . At the depth of 2523.6 m, the consumed power is 7.7 W.

The linear power–pressure dependence follows from the functional connection of the power with the density and dynamic viscosity of fluid in which the eccentric mass rotates. In 1934 White and Brenner [24] obtained the expression for the power consumption:

$$P = N_p \rho \omega^3 D^5, \quad (3)$$

where ρ is the fluid density, kg/m^3 ; ω is angular velocity, rad/s ; D is the eccentric mass diameter, m; N_p is the dimensionless number of power, or the Newton number [14, 16, 20, 21]. The functional

dependence between N_p , Reynolds number Re , Froude number Fr and geometrical dimensions of turbin and tank where rotation takes place is given in [25, 26]:

$$N_p = \frac{P}{\rho \omega^3 D^5} = k \left(\frac{\rho \omega D^2}{\mu} \right)^\alpha \left(\frac{\omega^2 D}{g} \right)^\beta f(l, w, T, c), \quad (4)$$

where k is the coefficient of proportionality; μ is the dynamic viscosity of fluid, Pa·s; α, β are the experimentally determined exponents; $f(l, w, T, c)$ is the functional connection between geometrical sizes of turbine and tank; l, w are the length and width of blade; T is the length of the tank; c is the clearance between the blade and the tank bottom.

Inasmuch as the density and dynamic viscosity of fluid changes with increasing pressure, at the same rotation frequency of eccentric mass, the number of power and the density will change by the law: $N_p(p) = 1.35 \cdot 10^{-3} p - 0.00214$, $\rho(p) = 0.48p + 998.2$. Placing $N_p(p)$ and $\rho(p)$ in (3) produces: $P(p) = 0.00016p^2 + 0.323p - 0.513$. Disregarding the quadratic term in the latter expression, we obtain the linear dependence: $P(p) = 0.323p - 0.513$.

In the producing well in the stratum U_1^1 in Verkh-Tarskoe oil field, the difference between the power intakes by the eccentric mass in fluid and water is 0.14 W. Such small difference is due to low viscosity of oil as compared with water and similarity of pressure distributions on the eccentric mass blade (Figure 3a).

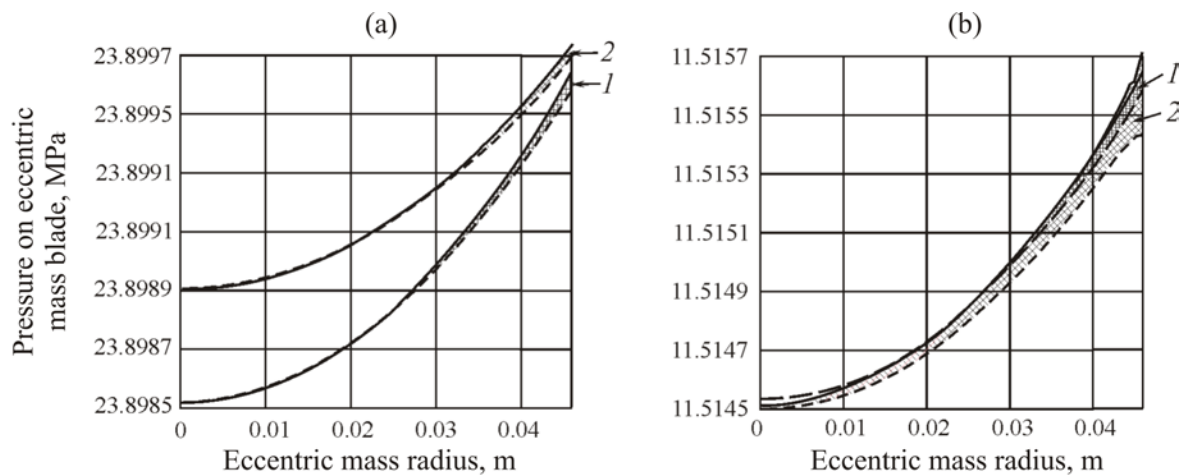


Figure 3. Distribution of pressure exerted by water (1) and oil (2) on the middlelegh section of eccentric mass blade: (a) Verkh-Tarskoe field oil (Novosibirsk Region, Russia)); (b) Tsagaan-Els field oil (East Gobi, Mongolia). Solid and dashed line show fluid pressure on the front and back sides of the blade, respectively.

For Tsagaan-Els field and well No. 1410, the difference in pressure distributions is higher for oil as against water (Figure 3b). Consequently, the power consumption is 2.7 times higher in oil than in water. The densities in water (1003.7 kg/m^3) and heavy oil (921.2 kg/m^3) differ insignificantly [23], and for this reason, the difference between values of pressure distribution on the eccentric mass blade ($r = 0 \text{ m}$) is also small—29 Pa.

5. Conclusions

The power consumption required to overcome water resistance in operation of downhole unbalance vibration source grows linearly with depth.

The unbalance source can operate in fields of light, low-viscosity and heavy viscous oil. In terms of Verkh-Tarskoe field of light and low-viscous oil in the stratum U_1^1 at the average depth of

occurrence ranging from 2455.6 to 2530.4 m, it is shown that overcoming of oil resistance in operation of downhole unbalance vibration source will consume 7.43 W additionally to 0.9 kW taken by the source. In Tsagaan-Els field of heavy viscous oil in productive stratum at a depth of 1170 m, 8.75 W of the motor net power will be consumed.

Acknowledgements

This work was carried out in the framework of the Basic Research Program, Project No 0321-2016-0005.

References

- [1] Dyblenko VP 2008 *Methods of Wave Stimulation of Scavenger Oil Reservoir. Review and Classification* Moscow: VNIIOENMG (in Russian)
- [2] Hua G, Falcone G, Teodoriu C and Morrison GL 2012 Comparison of multiphase pumping technologies for subsea and downhole applications *Oil and Gas Facilities* pp 36–46
- [3] Snarev AI 2010 *Design of Machines and Equipment for Oil and Gas Production: Educational and Training Aid* Moscow: Infra-Inzheneria (in Russian)
- [4] Kostrov S and Wooden W 2005 In seismic stimulation shows promise for revitalizing mature fields *Oil & Gas Journal* Vol 103 No 15 pp 43–49
- [5] Westermarck RV, Brett JF and Maloney DR 2002 Enhanced oil recovery with downhole vibration stimulation *SPE/DOE Thirteenth Symposium on Improved Oil Recovery* Tulsa, Oklahoma pp 1–8 DOI: doi.org/10.2118/67303-MS
- [6] Savchenko AV, Stupin VP et al 2016 Development of borehole unbalance vibrosources and test benches for their research *Proceedings of Interexpo GEO-Siberia-2016: International Scientific Conference* Vol 4 pp 3–7 Novosibirsk: SSGA (in Russian)
- [7] Tsupov MN and Savchenko AV 2016 Development of seismic vibration sources for rock mass treatment *Mashinovedenie* Vol 4 pp 62–67
- [8] Luo JY, Issa RI and Gosman AD 1994 Prediction of impeller induced flows in mixing vessels using multiple frames of reference *European Conference on Mixing—ICHEME Symp Series* UK: Univ. Cambridge No 136 pp 549–556
- [9] Tonello N, Eude Y, Meux B and Ferrand M 2017 Frozen rotor and sliding mesh models applied to the 3D Simulation of the Francis-99 Tokke turbine with Code_Saturne *IOP Conf. Series: Journal of Physics: Conf. Series* 782 pp 1–12 DOI: 10.1088/1742-6596/782/1/012009
- [10] Giorgi MG, Donato T et al 2017 Numerical investigation of the performance of contra-rotating propellers for a remotely piloted aerial vehicle *Proc. 72nd Conf. of the Italian Thermal Machines Engineering Association* Lecce, Italy pp 1101–1018
- [11] Kim Ch, Park J, Kim D and Baek J 2016 Numerical analysis on non-equilibrium steam condensing flow in rotating machinery *ASME 28th Symposium on Fluid Machinery* Washington pp 1–11 DOI: 10.1115/FEDSM2016-7588
- [12] Lopes Jr GB, Gómez LC and Bock EGP 2016 Mesh independency analyses and grid density estimation for ventricular assist devices in Multiple Reference Frames simulations *Technische Mechanik* Vol 36 No 3 pp 190–198
- [13] Stein P, Pfoster Ch et al 2015 Computational fluid dynamics modeling of low pressure steam turbine radial diffuser flow by using a novel multiple mixing plane based coupling—Simulation and validation *J. Eng. Gas Turbines Power* Vol 138 No 4 DOI:10.1115/1.4031388
- [14] Gülich JF 2010 *Centrifugal Pumps* Springer-Verlag Berlin Heidelberg
- [15] Rielly CD and Gimbum J 2019 *Computational fluid mixing Food Mixing. Principles and Applications* Chichester: Wiley Blackwell pp 125–174
- [16] Kresta SM, Etchells III et al 2016 *Advances in Industrial Mixing: A Companion to the Handbook of Industrial Mixing* John Wiley & Sons
- [17] Schlichting H and Gersten K 2017 *Boundary-Layer Theory* Springer-Verlag Berlin Heidelberg

- [18] Charny IA 1951 *Unsteady Motion of Real Liquid in Pipes* Leningrad: Izd. Tekhniko-Tekhnich. Lit. (in Russian)
- [19] Aleksandrov AA and Grigor'ev BA 1999 Handbook: Tables of thermophysical Properties of Water and Water Vapor Moscow: MEI (in Russian)
- [20] Edward LP, Atiemo-Obeng VA and Kresta SM 2004 Handbook of Industrial Mixing: Science and Practice New Jersey: John Wiley & Sons
- [21] Cengel YA and Cimbala JM *Fluid Mechanics* McGraw Hill Education
- [22] Antonov DA 2002 Efficiency of the Use of Oil Gas in Verkh-Tarskoe Oil Field (Novosibirsk Region) Bachelor's Thesis (in Russian)
- [23] Gehrehlmaa T 2010 Investigation of the processes of biodegradation of viscous oils in Mongolia for creating methods for increasing oil recovery and reclamation of oil-contaminated soils *Theses of Candidate of Chemical Sciences Dissertation* Tomsk (in Russian)
- [24] White AM and Brenner E 1934 Studies in Agitation vs the correlation of power studies data *Trans. Ame. Ins. Chem. Eng.* Vol. 30 pp. 585–579
- [25] Bates RL, Fondy PL and Corpstein RR 1963 Examination of some geometric parameters of impeller power *Industrial & Engineering Chemistry Process Design and Development* Vol 2 No 4 pp 310–314 DOI: 10.1021/i260008a011
- [26] Chudacek MW 1985 Impeller power numbers and impeller flow numbers in profiled bottom tanks *Industrial & Engineering Chemistry Process Design and Development* Vol 24 No 3 pp 858–867 DOI: 10.1021/i200030a056V